Journal of Saudi Chemical Society (2015) **xxx**, xxx–xxx

King Saud University

Journal of Saudi Chemical Society

www.ksu.edu.sa
www.sciencedirect.com

ORIGINAL ARTICLE

Butea monosperma bark extract mediated green synthesis of silver nanoparticles: Characterization and biomedical applications

Sutanuka Pattanayak [a], Md. Masud Rahaman Mollick [b], Dipanwita Maity [b], Sharmila Chakraborty [c], Sandeep Kumar Dash [d], Sourav Chattopadhyay [d], Somenath Roy [d], Dipankar Chattopadhyay [b], Mukut Chakraborty [a,*]

[a] *Department of Chemistry, West Bengal State University, Barasat, Kolkata 700126, West Bengal, India*
[b] *Department of Polymer Science & Technology, University of Calcutta, 92, A.P.C. Road, Kolkata 700009, West Bengal, India*
[c] *Department of Microbiology, Sammilani Mahavidyalaya, Baghajatin, E.M. Bypass, Santoshpur, Kolkata 700094, West Bengal, India*
[d] *Immunology and Microbiology Laboratory, Department of Human Physiology with Community Health, Vidyasagar University, Midnapore 721 102, West Bengal, India*

Received 19 August 2015; revised 24 November 2015; accepted 30 November 2015

KEYWORDS

Butea monosperma;
Green route;
Silver nanoparticles;
Antibacterial;
Anticancer

Abstract The work deals with an environmentally benign process for the synthesis of silver nanoparticle using *Butea monosperma* bark extract which is used both as a reducing as well as capping agent at room temperature. The reaction mixture turned brownish yellow after about 24 h and an intense surface plasmon resonance (SPR) band at around 424 nm clearly indicates the formation of silver nanoparticles. Fourier transform-Infrared (FT-IR) spectroscopy showed that the nanoparticles were capped with compounds present in the plant extract. Formation of crystalline fcc silver nanoparticles is analysed by XRD data and the SAED pattern obtained also confirms the crystalline behaviour of the Ag nanoparticles. The size and morphology of these nanoparticles were studied using High Resolution Transmission Electron Microscopy (HRTEM) which showed that the nanoparticles had an average dimension of ~35 nm. A larger DLS data of ~98 nm shows the presence of the stabilizer on the nanoparticles surface. The bio-synthesized silver nanoparticles revealed potent antibacterial activity against human bacteria of both Gram types. In addition these biologically synthesized nanoparticles also proved to exhibit excellent cytotoxic effect on human myeloid leukemia cell line, KG-1A with IC_{50} value of 11.47 μg/mL.

* Corresponding author.
Peer review under responsibility of King Saud University.

ELSEVIER Production and hosting by Elsevier

1. Introduction

Nanomaterials especially the nano-scale noble metals attract a lot of attention due to their remarkable difference in structural

http://dx.doi.org/10.1016/j.jscs.2015.11.004
1319-6103 © 2015 King Saud University. Production and hosting by Elsevier B.V.

and physical properties compared to those of atoms, molecules and bulk materials of the same element [1]. In recent years, development of this field gave rise to a new technology known as 'Nanotechnology' that provides us with a technology and a tool for investigation and its application to biological systems at the nanoscale. Nanostructured materials exhibit various aspects of interesting features viz, optical, catalytic etc. that greatly depends on the size and shape of nanoparticles. Metal nanoparticles have enormous utility in electrochemical, electro-analytical and bio-electrochemical applications owing to their extraordinary electro-catalytic activity [2]. Hence, nanotechnology is an emerging field in the area of interdisciplinary research, having application in biology [3]. Conventional route of nanoparticle synthesis by physical and chemical methods are environmentally hazardous, technically laborious and financially expensive. Many researchers have explored different technological approaches for the synthesis of nano-materials. Silver nanoparticles produced by chemical, electrochemical, radiation, photochemical methods, Langmuir–Blodgett and biological techniques have also been reported [4]. However, these reports on the synthesis of silver nanoparticles use hazardous chemicals, have low material conversions, high energy requirements and consist of difficult and elaborate purification steps. Researchers have since initiated the synthesis of nanoparticles using green methods [5]. The biological effectiveness of bio-nanoparticles synthesized using green methods increases due to an increase in the surface area and hence have greater catalytic activity [6]. The possibility of using microbes and plant materials as nano-precursors has also been studied [7]. Since then, various microorganisms and plants have been utilised for the synthesis of nanomaterials. Different types of nanomaterials like copper [8], zinc [8], titanium [8], magnesium [9], gold [9], alginate [10] and silver [11,12] etc. have been synthesized using the above. Silver exhibits low toxicity in humans and has a range of diverse applications [13]. Currently, silver-based dressings are extensively used to treat infections in open wounds and chronic ulcers [14]. While various hypothesis persist regarding the mechanism of antimicrobial or antibacterial activity of silver nanoparticles in the cell membrane, the general perception is that the leakage of intracellular substances due to rupture of the cell structure eventually causes cell death [15]. Recently, Palza [16] have reviewed the antimicrobial effect of metal nanoparticles on different polymers.

The surface plasmon resonance and large effective scattering cross section of individual silver nanoparticles make them ideal candidates for molecular labeling where phenomena such as surface enhanced Raman scattering (SERS) are exploited [17]. In addition, silver nanoparticles play a significant role in the field of biology and medicine due to its attractive physicochemical properties. Silver nanoparticles are found to possess anti-inflammatory, anti-viral, anti-angiogenesis and anti-platelet activity and exhibits cytotoxicity against cancer cells [18,19].

In vitro studies is an important tool to assess the mechanisms of toxicity caused by nanomaterials. Researchers have focused on the biogenic synthesis of silver nanoparticles using *Sesbania grandiflora* (L.) and its use for the in vitro cytotoxicity analysis of breast cancer cell lines (MCF-7) [20]. The effect of colloidal silver on MCF7 human breast cancer cells has also been observed [21]. The synthesis of Ag NPs using biological system and evaluation of its potential toxicity and general mechanism of its action on MDA-MB-231 human breast cancer cells are reported [22]. Different cell types have been considered for cytotoxicity of Ag NPs, including NIH 3T3 fibroblast cells [23], HeLa cells [24] and human glioblastoma cells [25]. It is also reported that Ag NPs, not only disrupts normal cellular function but also affects the membrane integrity, inducing various apoptotic signaling genes of the mammalian cells leading to programmed cell death [26]. The mechanisms for Ag NPs induced toxicity is interrelated with mitochondrial damage, oxidative stress, DNA damage and induction of apoptosis [27]. Now a days' leukemia has become a life threatening hematological disorder characterized by uncontrolled cell growth due to abnormal cellular metabolism. Worldwide ever increasing death rate of patients suffering from different types of leukemia and severe failure of conventional and traditional chemotherapy has attracted the attention of many researchers for alternative management to combat this disease. To date, numerous methods have been employed for the synthesis of Ag NPs ranging from chemical [28], radiation [29], electrochemical [30] and photochemical methods [31]. Recently, biological synthesis of nanoparticles in a sustainable mode finds extensive use in biomedical applications [32]. In a recent study, the cytotoxic activity of *Melia azedarach* was showed against human lung adenocarcinoma cell lines [33].

Toxic impact of traditional chemotherapeutics and drug resistance property creates an urgent need for development of alternative treatment for cancer. Leukemia, a type of cancer of the white blood cells or bone marrow and is manifested by an abnormal increase of immature white blood cells called "blasts". Acute myelogenous leukemia (AML) is a fast growing fatal form of leukemia responsible for production of non-functional immature white blood cells which initiates in bone marrow cells and quickly spreads into the blood system [34]. Extensive studies have been carried out to develop new agents for the treatment of AML, however the combination of AraC and anthracyclines is still considered as the most effective for AML therapy. Silver nanoparticles have subsequently been considered as one of the potential agent in bio-medical applications with high commercial interests [35]. However, the toxicity of the said nanoparticles towards normal cells should be overcome for its effective application in anti-cancer research. Ag NPs developed from bio-reduction methods show minimal toxicological impacts towards normal cells [36].

Different microorganisms like bacteria [37], fungi [38] and yeast [39] have been used for the biosynthesis of silver nanoparticles. The possibility of using plant materials for the synthesis of nano-scale metals was first reported by Gardea-Torresdey et al. [40,41]. Further, synthesis of silver nanoparticles using extracts of various plants like *Aloe vera* [42], *Cinnamon zeylanicum* [43], *Carica papaya* [44], *Desmodium triflorum* [45], *Ocimum sanctum* [46] are also reported. Sun-dried *Cinnamon camphora* leaf for the synthesis of nano-sized noble metals Ag and Au at ambient conditions has also been demonstrated previously [47]. So, the potential of plants as biological precursor for the synthesis of nanoparticle is currently under extensive study [48].

Here, we have chosen another unique plant *Butea monosperma* as our biological material for nanoparticle synthesis. It is widely available in the state of West Bengal, mainly in Purulia district. We have extracted the bark of this plant and used it as a reducing as well as capping agent for the synthesis

Please cite this article in press as: S. Pattanayak et al. *Butea monosperma* bark extract mediated green synthesis of silver nanoparticles: Characterization and biomedical applications, Journal of Saudi Chemical Society (2015), http://dx.doi.org/10.1016/j.jscs.2015.11.004

of silver nanoparticles. The present investigation deals with *B. monosperma* bark extract mediated synthesis and characterization of silver nanoparticles as well as their biomedical applications Characterization and biomedical applications.

2. Materials and methods

All the chemicals used in the present study were of highest purity and were used as received. Silver nitrate ($AgNO_3$), GR was purchased from Merck (Mumbai, India), KBr from Sigma, Nutrient agar from Hi Media. Triple distilled water was used throughout for the synthesis. Barks of *B. monosperma* plant were collected from Purulia district of West Bengal, India.

2.1. Preparation of B. monosperma bark extract

The collected bark of *B. monosperma* plant was first rinsed thoroughly under tap water and then with triple distilled water to remove all impurities. This was then air dried and thoroughly grinded to form a uniform mixture, which was used throughout the study. About 0.29 g of this mixture was soaked in triple distilled water taken in a 100 mL beaker to obtain ~1.2% (w/v) concentrated extract. Filtration was done after 24 h with the help of Whatman filter paper no. 42 and a bright orange coloured extract was finally obtained. This was stored in a refrigerator for further use.

2.2. Synthesis of silver nanoparticles (Ag NPs)

For the biosynthesis of silver nanoparticles, 1 mL of bark extract was mixed with 6 mL of 1 mM $AgNO_3$ solution at room temperature and was kept in dark for 24 h. After the stipulated time, a brown–yellow colour solution was obtained. The colour of the solution, due to the formation of Ag NPs was confirmed by UV–Vis studies. The purification of Ag NPs was done after centrifugation and repeated washings and the concentrated slurry was collected after discarding the supernatant. The collected silver nanoparticles were allowed to air dry.

2.3. Characterization of silver nanoparticles (Ag NPs)

The formation of silver nanoparticles was confirmed by the presence of typical SPR band in the UV–Vis spectrum. To examine the stability of the biosynthesized silver nanoparticles, the brown–yellow solution was kept in the refrigerator and the spectra recorded after different time intervals. The spectra were recorded on double beam spectrophotometer (Perkin Elmer Lambda 25) in the range 200–800 nm at a resolution of 1 nm.

The morphology of Ag NPs was examined with the help of HR Transmission Electron Microscopy (HRTEM) equipped with X-ray energy dispersive spectrometer (EDX). A small drop of dispersed Ag NP solution was cast over a 300 mesh carbon coated copper grid and then left for air drying. HRTEM and Selected Area Electron Diffraction (SAED) images were taken on JEOL JEM 2100 operated at an accelerating voltage of 200 kV.

Dynamic Light Scattering (DLS) measurements were carried out to measure the size of a nanoparticle including their surroundings. The average hydrodynamic diameter was measured by a Zetasizer Nano-ZS90 analyser System (Malvern Inc.).

The purified, dried, solid silver nanoparticles powder was subjected to Fourier transform-Infrared (FT-IR) spectroscopic measurement. These measurements were carried out on a Perkin Elmer spectrum one instrument in the diffuse reflectance mode at a resolution of 4 cm^{-1} using KBr pellets. The finely powdered dried bark sample was mixed with KBr to obtain it in the pelletized form. The pellets were subjected to FT-IR spectroscopic measurement.

The crystallinity pattern of the synthesized Ag NPs was confirmed by X-Ray Diffraction (XRD) measurements. It was carried out on a PANalytical: XPERT-PRO equipment using step scan technique and was scanned in the range 30–120 (2θ) degrees.

2.4. Antibacterial activity of Ag NPs

It has been reported that freshly synthesized silver nanoparticles have better antimicrobial properties [49]. The antibacterial activity of freshly synthesized bark extract mediated Ag NPs was assessed against both Gram positive (*Bacillus subtilis*) and Gram negative (*Escherichia coli*) bacteria by agar diffusion method as illustrated earlier [50]. The bacterial cultures were grown in Nutrient agar (NA) medium that contained peptone (1%), beef extract (1%) and NaCl (1%) with pH 6.8. Sterile Nutrient agar petri plates were prepared and 0.1 mL of the overnight grown bacterial culture was spread on the solidified agar plates evenly with the help of a glass spreader. After allowing sufficient time for adsorption of the bacterial cells, wells were made on the solidified agar using a cork borer of suitable diameter so that three wells can be made on a plate. Centrifuged and thoroughly washed silver nanoparticles were added into the wells. 50 µl of each compound of concentration 100 µg/mL was poured into each well using a micropipette. Both triple distilled water and the extract (same concentration as used in synthesis) were used here as control. The plates were incubated at 37 °C for 24 h. On the next day the diameter of zones of inhibition were measured and recorded. For each zone at least three readings were taken.

2.5. Anti cancerous activity of silver nanoparticles

2.5.1. Culture media and chemicals

3-(4,5-dimethyl-2-thiazolyl)-2,5-diphenyl-2H-tetrazolium bromide (MTT reagent), Ethidium bromide, Acridine Orange, 4′,6-diamidino-2-phenylindole dihydrochloride (DAPI) were procured from Sigma (St. Louis, MO, USA). Minimum Essential Medium (MEM), RPMI 1640, fetal bovine serum (FBS), penicillin, streptomycin, sodium chloride (NaCl), sodium carbonate (Na_2CO_3), sucrose, Hanks balanced salt solution, and ethylene diamine tetra acetate (EDTA), dimethyl sulfoxide (DMSO) were purchased from Himedia, India. Tris-HCl, Tris buffer, KH_2PO_4, K_2HPO_4, HCl, alcohol and other chemicals were procured from Merck Ltd., Mumbai, India. All other chemicals of the highest purity grade were purchased from Merck Ltd., SRL Pvt. Ltd., Mumbai.

2.5.2. Cell lines culture and maintenance

KG-1A cell line was cultivated for in vitro experiments. This cell line was obtained from the National Centre for Cell Sciences, Pune, India. It was cultured in RPMI 1640 medium supplemented with 10% fetal calf serum, 100 units/mL

Please cite this article in press as: S. Pattanayak et al. *Butea monosperma* bark extract mediated green synthesis of silver nanoparticles: Characterization and biomedical applications, Journal of Saudi Chemical Society (2015), http://dx.doi.org/10.1016/j.jscs.2015.11.004

penicillin and 100 μg/mL streptomycin, 4 mM L-glutamine under 5% CO_2, and 95% humidified atmosphere at 37 °C. Cells were cultured and maintained in logarithmic growth phase until the number of cells reached 1.0×10^6 cells/mL.

2.5.3. Preparation of drug

Several doses of Ag NPs (1, 5, 10, 25, 50 and 100 μg/mL) were prepared using sterile phosphate-buffered saline (pH 7.4). After dispersion it was scanned in UV–Vis spectrophotometer (Fig. S1) and a High Resolution Transmission Electron Microscopic (HRTEM) image (Fig. S2) was taken. From these results, it was proved that the Ag NPs were stable at pH 7.4. A 10 mg/mL stock of Ag NPs was prepared by dissolving 10 mg of Ag NPs in PBS and sonicated for 15 min. It was then serially diluted with RPMI media to prepare working concentrations. In this study, all these doses were charged against cancer cell lines for evaluation of in vitro anticancer activity.

2.5.4. Experimental design

KG-1A cells were treated with different concentration of Ag NPs (1, 5, 10, 25, 50 and 100 μg/mL) for 24 h. The KG-1A cells were divided into 6 groups. Each group contained 6 petridishes. In every set of treatment, cell numbers were maintained to 2×10^6 cells/petridish. The following groups were considered for the experiment and cultured for 24 h:

Group I: control i.e., cells + culture media, Group II: cells + 1 μg/mL Ag NPs in culture media, Group III: cells + 5 μg/mL Ag NPs in culture media, Group IV: cells + 10 μg/mL Ag NPs in culture media, Group V: cells + 25 μg/mL Ag NPs in culture media, Group VI: cells + 50 μg/mL Ag NPs in culture media. Group VI: cells + 100 μg/mL Ag NPs in culture media.

After 24 h of treatment the cells were collected from the petridishes separately and centrifuged at 2200 RPM for 10 min at 4 °C to separate the cells and the supernatant medium [51]. The cells were then washed twice with 1× PBS (50 mM), pH 7.4. Intact cells were used for determination of cell viability, ROS and different microscopic observations.

2.5.5. In vitro cytotoxicity assay

The cytotoxicity of silver nanoparticles was quantitatively measured by a non-radioactive, colorimetric assay systems using tetrazolium salt, 3-[4,5-dimethylthiazol-2-yl]-2,5-diphe nil-tetrazolium bromide (MTT) [51]. Briefly, 5 mg/mL MTT solution was prepared by dissolving MTT in phosphate-buffered saline and filtered to remove the small amount of insoluble residue present in some batches. Then MTT solution was added directly to all microtitre plate wells (10 μL per 100 μL medium) containing cells (1×10^5/well) and complete growth medium, with or without the nano particle. It was then incubated for 4 h at 37 °C to metabolize the MTT to formazan. Subsequently, the supernatant was aspirated and 100 μL of HCl-isopropanolic solution (1:1) was added to each culture plate and mixed thoroughly to dissolve the dark blue formazan crystals. The optical density (OD) of the samples was measured on ELISA reader (BIO-RAD, Model 550, Tokyo, Japan) using test and reference wavelengths of 570 and 630 nm, respectively. The percentage of proliferation was calculated by using the following equation:

$$\% \text{ Proliferation} = [OD_{sample} - OD_{control}] \times 100/OD_{control}$$

2.5.6. Calculation of IC_{50} value

The concentration required for 50% inhibition of viability (IC_{50}) was determined graphically. Multiple linear regressions were used to compare data using Statistica version 5.0 (Statsoft, India) software package.

2.5.7. Intracellular ROS measurement

ROS measurement was performed using H_2DCFDA according to the standard method [52]. In brief, KG-1A cell lines were treated with Ag NPs at 11.47 μg/mL for 24 h. After treatment schedule cells were washed with culture media followed by incubation with 1 μg/mL H_2DCFDA for 30 min at 37 °C. Then the cells were washed three times with fresh culture media. DCF fluorescence was determined at 485 nm excitation and 520 nm emission using a Hitachi F-7000 Fluorescence Spectrophotometer and was also observed by fluorescence microscopy (NIKON ECLIPSE LV100POL). All measurements were done in triplicate.

2.5.8. Pre-treatment with N-acetyl-L-cysteine

To determine the role of ROS in NP-induced cell death, KG-1A cells were seeded in a 96-well plate at 0.2 mL per well at a concentration of 2×10^6 cells/mL. A stock solution of N-acetyl-L-cysteine (NAC; Sigma–Aldrich) was made with sterile water and added to cells at 5 and 10 mM for 4 h [52]. After NAC pretreatment, cells were cultured with Ag NPs for 24 h. Viability was determined by the MTT method.

2.5.9. Cellular morphology analysis by Acridine orange (AO)–ethidium bromide (EtBr) double staining

To confirm the probable pathway of cell death we analyzed the cells by AO – EtBr double staining method. A number of 2×10^4 KG-1A cells were seeded into each well of a 6-well plate and incubated for 24 h at 37 °C in a humidified, 5% CO_2 atmosphere. Ag NPs at 11.47 μg/mL dose was then added into the well and left for 24 h. After incubation, the cells were washed once with phosphate buffer saline (PBS). Ten microlitres of the cells were then put on a glass slide and mixed with 10 μl of acridine orange (50 μg/mL) and ethidium bromide (50 μg/mL). The cells were viewed under a fluorescence microscope (NIKON ECLIPSE LV100POL) with 400× magnification [53].

2.5.10. Assessment of nuclear morphological changes by DAPI staining

The DAPI staining was performed according to the laboratory standard method [54]. For DAPI staining, all the test cells were seeded into six well plates. A number of 2×10^5 cells/mL were treated with or without Ag NPs (0 and 11.47 μg/mL) for 24 h and were then isolated for DAPI staining. After treatment, the cells were fixed with 2.5% glutaraldehyde for 15 min, permeabilized with 0.1% Triton X-100 and stained with 1 mg/mL DAPI for 5 min at 37 °C. The cells were then washed with PBS and examined by fluorescence microscopy (NIKON ECLIPSE LV100POL).

2.5.11. Statistical analysis

All the parameters were repeated at least three times. The data were expressed as mean ± SEM, $n = 06$. Comparisons between the means of control and treated group were made

by one-way ANOVA test (using a statistical package, Origin 6.1, Northampton, MA 01060 USA) with multiple comparison t tests, $p < 0.05$ as a limit of significance.

3. Results and discussions

3.1. Ultraviolet–Visible (UV–Vis) spectroscopic analysis

Brownish yellow coloured solution of silver nanoparticles was obtained from colourless $AgNO_3$ solution and the NP formation was established through UV–Visible spectrophotometry. The appearance of the colour was due to the excitation of the surface plasmon vibrations, typical of Ag NPs having λ_{max} values which are reported in the visible range of 400–450 nm [55]. The UV–Vis spectrum of the samples are shown in Fig. 1 where the spectra of the stabilized Ag NPs and the extract are denoted by 'a' and 'b' respectively. The colour of the two solutions could be easily distinguished from the inset picture. The peak at 279 nm in both the spectra in Fig. 1 confirmed the presence of amino acid residues [56,57]. The amino acid residues present in the extract presumably play a vital role for reduction as well as stabilization of nanoparticles [58]. Spectrum 'a' in Fig. 1 clearly exhibits the SPR band of silver nanoparticles at 424 nm and the peak at 279 nm is also present, indicating the presence of the amino acid residues in the synthesized Ag NPs.

3.2. Analysis of stability of nanoparticles

The stability of synthesized nanoparticles is strictly dependent on the degree of aggregation, which can be monitored by the change in the SPR band. Silver nanoparticles prepared in this way were quite stable without any reasonable aggregation. Fig. S3 depicts this observation quite satisfactorily. In this figure, the spectra 'a' and 'b' indicated the SPR band of extract mediated silver nanoparticles solution just after synthesis and after 60 days. The solution containing the nanoparticles was quite stable even after two months though the SPR absorbance peak position has been slightly red shifted (Fig. S3b). This slight decrease in intensity as well as shift in wavelength amongst spectra 'a' and 'b' was probably due to some aggregation of nanoparticles [59,60]. Analysing these spectroscopic results we can suggest that the Ag NPs are quite stable at room temperature and does not exhibit any considerable aggregation.

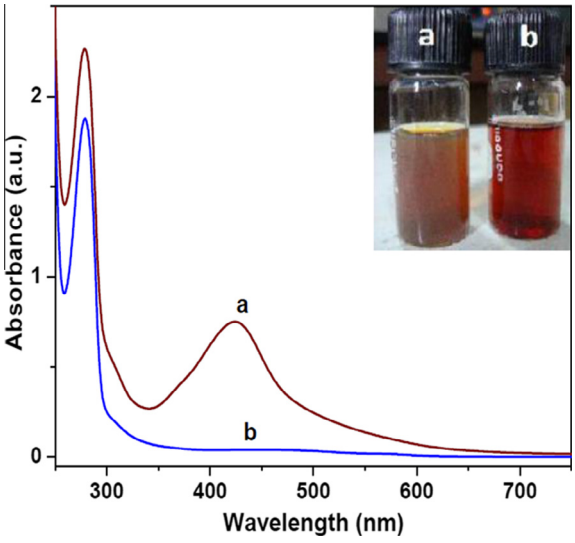

Figure 1 UV–Vis spectra of (a) *Butea monosperma* bark extract reduced silver nanoparticles (b) *Butea monosperma* bark extract solution. The figure in the inset shows the color of (a) synthesized silver nanoparticles (b) *Butea monosperma* bark extract solution.

3.3. High Resolution Transmission Electron Microscopy (HRTEM) study

The size and shape of the nanoparticles formed using the biomolecules available in the extract of *B. monosperma* bark was studied using the High Resolution Transmission Electron Microscopy (HRTEM) technique. Fig. 2a depicts the HRTEM image of biosynthesized silver nanoparticles showing the lattice fringes quite clearly. The nearly spherical shaped particles with smooth edges are also quite distinct from this image. From Fig. 2b and c, it is shown that most of the particles are nearly spherical in shape and the size of the particles range between 18 nm and 50 nm with an average size of ~35 nm. There are a few traces of Ag NPs clusters which may contribute for the variation in particle size. On close observation, we can clearly see that the clusters have been formed when the individual particles have clustered together. The calculation of the size of these nanoparticles was done based on the size obtained from the HRTEM images. The SAED pattern of the synthesized particles is also given in the inset of Fig. 2c, which clearly depicts that the Ag NPs are crystalline in nature.

The energy dispersive X-ray analysis (EDX) shown in Fig. 2d revealed a strong signal of silver and again confirmed the formation of Ag NPs. Metallic silver nanocrystals generally show typical optical absorption peak at ~3 keV which is typical for the absorption of metallic silver [61]. Peaks of carbon and copper were also obtained due to the carbon coated copper grid.

3.4. Dynamic Light Scattering (DLS) study

The average diameter of bark extract mediated Ag NPs was measured using DLS. Fig. S4 showed the average particles size distribution of Ag NPs having a mean particle size of ~98.28 nm. The difference between the diameter values obtained from HRTEM and DLS measurement was mainly due to the process involved in the sample preparation. The particle size determined by HRTEM represents the actual diameter of the nanoparticles as it was measured at the dry state of the sample, whereas by the laser light scattering (DLS) method the hydrodynamic diameter (hydrated state) of nanoparticles were obtained; therefore, the nanoparticles will have a larger hydrodynamic volume due to solvent effects in the hydrated state [62].

3.5. Fourier transform-Infrared (FT-IR) spectroscopic analysis

To characterize and identify the biomolecules that were bound specifically on the synthesized Ag NPs, FT-IR spectroscopic analysis was utilized. The spectrum obtained for *B. monosperma* bark extract (Fig. 3a) displayed a number of peaks

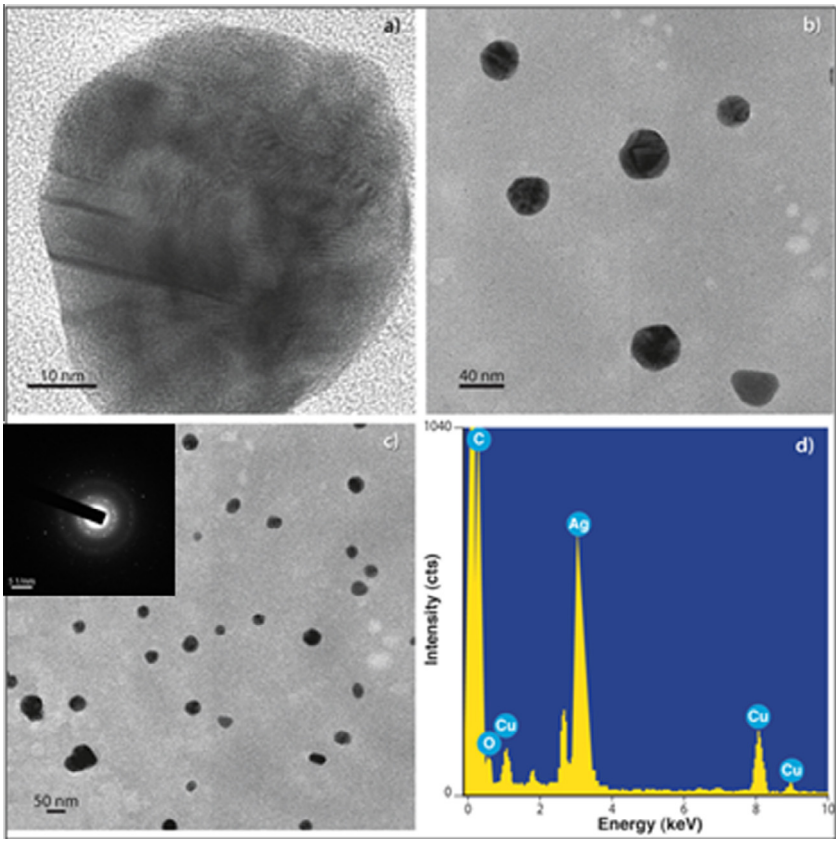

Figure 2 (a) HRTEM image of a single silver nanoparticle with lattice fringes, (b) HRTEM micrograph images of spherical silver nanoparticles at different grid location, (c) HRTEM micrograph images of spherical silver nanoparticles at different grid location along with SAED pattern in inset (d) EDX spectrum of Ag NP from HRTEM.

reflecting its complex nature. The peak at 3456 cm^{-1} resulted from stretching vibrations of the —NH bond of the peptide linkages. The peaks at 2947 and 2896 cm^{-1} is assigned to the stretching vibrations of the $-CH_2$ and $-CH_3$ functional groups. The peak at 1758 cm^{-1} indicates the presence of carbonyl (C═O) originating from carboxylic acid group. The interesting thing was that the 1758 cm^{-1} peak was absent in the spectra recorded for the extract stabilized Ag NPs (Fig 3a). So, we presume that the absence of the peak is attributed to the fact that the carboxylic acid group is absent in the nanoparticle and hence, plays a role in the reduction of Ag^+ to Ag^0. The band found at 1642 cm^{-1} for the extract is assigned to the amide I group of proteins present in the amino acid residues in the plant extract. However, after capping of the silver nanoparticles the band appears at 1608 cm^{-1} which gives evidence of the fact that the protein residues present in the extract play a part in the stabilization of Ag NPs. In the case of extract stabilized nanoparticles, the peak at 3456 is shifted to 3420 cm^{-1}, bands from 1467 to 1442 cm^{-1} and 1398–1380 cm^{-1} implying the binding of silver metal with hydroxyl and carboxylate groups of the protein residues. The spectra also illustrated a prominent shift in the wavenumbers corresponding to amide I group of proteins, (from 1642 to 1608 cm^{-1}) signifying that the groups actively participate in the stabilization process of the nanoparticles. The results obtained above are similar to previous reports [63,64]. Shifting of alkyl C—H bands from 2947 to 2930 cm^{-1} and from 2896 to 2843 cm^{-1} also confirmed the plausible interaction between plant extract bio compounds and Ag NPs. The peaks at 1336 and 1083 cm^{-1} in the extract confirmed the presence of tryptophan indole ring [65]. Shifting of these peaks and decreasing band intensity revealed the fact that tryptophan residues of the protein also play a role in the reduction and stabilization of Ag NPs. The reasonable shifts in the peak positions indicate that the different phytochemicals present in the *B. monosperma* bark extract are present in the extract stabilized nanoparticles.

3.6. X-ray diffraction (XRD) study

X-ray diffraction was carried out to confirm the crystalline nature of the silver nanoparticles formed. Fig. 3b shows the XRD pattern of the Ag NPs which had a number of Bragg reflections that may be indexed on the basis of face-centred cubic structure of silver. A comparison of the XRD spectrum with the standard data confirmed that the silver metal formed in our experiments were in the form of fcc crystalline lattice as evidenced by the peaks at 2θ values of 38.44°, 44.57°, 64.78°, 77.64°, 81.80°, 110.87° and 115.07° representing the (1 1 1), (2 0 0), (2 2 0), (3 1 1), (2 2 2), (3 3 1) and (4 2 0) Bragg's reflections of the face-centred cubic structure of silver and these planes correspond to the standard JCPDS file no. 04-0783.

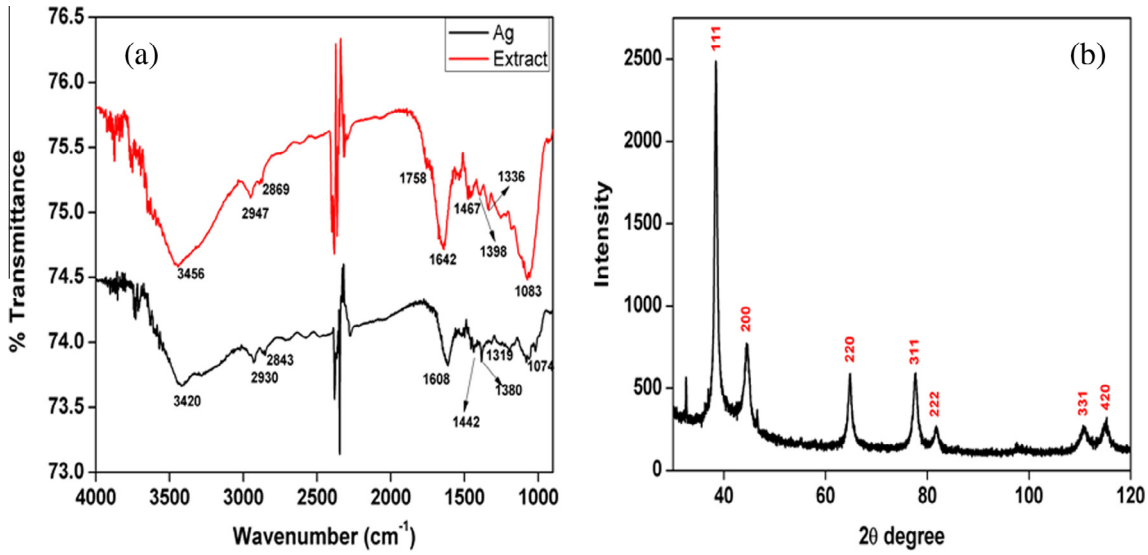

Figure 3 (a) FTIR spectra of *Butea monosperma* bark extract and extract stabilized Ag NP, (b) XRD pattern of silver nanoparticles synthesized from barks of *B. monosperma*.

3.7. Antibacterial activity of synthesized silver nanoparticles

The antibacterial activity of Ag NPs, $AgNO_3$, *B. monosperma* bark extract and triple distilled water as control were assessed and the results have been represented in Table S1. Ag NPs (50 μL at a concentration of 100 μg/mL) had shown zone of inhibition of diameter of about 17 mm for *E.* coli and 16 mm zone diameter for *B.* subtilis as shown in Table S1 and in Figs. S5 and S6. *B. monosperma* bark extract and triple distilled water used as control in this experiment and did not show any zone of inhibition. The zone diameters observed with $AgNO_3$ solution, used for the nanoparticles synthesis, was more when compared to Ag NP. From this comparative study it can be concluded that silver nanoparticles synthesized from the extract had good antibacterial activity. The smaller concentration (nanorange) of Ag NPs is much safer on cells compared to conventional $AgNO_3$ solution and is hence more applicable for usable purposes [5]. In this context, it is to be mentioned that though $AgNO_3$ gives larger zones of inhibition a high concentration of Ag is harmful for both the consumer and the microbes. Thus, we can say that the Ag NPs prepared have good antibacterial activity and can be used as potent therapeutic agents at much smaller concentrations compared to conventional $AgNO_3$ solution. It has also been reported that the changes observed in the membrane structure of bacterial cell wall due to the action of Ag NPs is caused by the interaction of embedded silver nanoparticles resulting in increased membrane permeability and consequently, death of the bacteria [66]. In conclusion, *B. monosperma* bark extract is capable for the green and eco-friendly synthesis of Ag nanoparticles which can be used as a potential entrant species having antibacterial applications.

3.8. In vitro cell viability assay

The anticancer activity of the Ag NPs was measured towards KG-1A cell lines in vitro side by side toxic effects of the particles was tested on human PBMCs. KG-1A cells and PBMCs were exposed to different concentrations (0, 1, 5, 10, 25, 50 and 100 μg/mL) of Ag NPs for 24 h and the cell viability was measured using MTT assay (Fig. 4a). The results show that, the Ag NPs decreased the viability of KG-1A by 12.69%, 38.59%, 61.59%, 84.07%, 89.45% and 97.53% at 1, 5, 10, 25, 50 and 100 μg/mL doses respectively. In the same line of treatment it decreases the viability of PBMCs by 2.66%, 21.53%, 53.55%, 54.60%, 62.39% and 70.053% respectively. The IC_{50} value of Ag NPs against KG-1A and PBMCs were determined using Statistica version 5.0 (Statsoft, India) software package. From this statistical calculation it was found that in KG-1A cells the IC_{50} value of Ag NPs was 11.47 μg/mL and 43.18 μg/mL in case of human PBMCs. As the significantly lower IC_{50} value was noted for leukemic cells, hence the further experiments were carried out using this dose only.

3.9. Cellular ROS level

The potentiality of Ag NPs to induce oxidative stress was assessed by measuring the intracellular ROS level. KG-1A cells exposed to Ag NPs for 24 h showed increased ROS formation as evidenced by increased DCF fluorescence intensity. Fig. 4b shows that the Ag NPs significantly ($p < 0.05$) induced the intracellular ROS production in KG-1A cells. It was found from our study that ROS generation level was increased by 4.203 fold in KG-1A cells at the effective dose (IC_{50}). From fluorescence microscopic images the higher green colouration in KG-1A cells treated with Ag NPs provides the visual evidence of higher ROS generation (Fig. 4d) compared to untreated cells (Fig. 4c).

Earlier reports showed that Ag NPs elevates the formation of intracellular ROS and reduction in ATP content. ROS are considered as molecules or ions containing unpaired electrons and being a free radical it is highly active and shows important role in cell signalling, leading to oxidative cell damage [25]. In normal cell, cellular glutathione effectively scavenges ROS, produces in minimal amounts during metabolic process and thereby maintain cellular normal behaviour. In the present

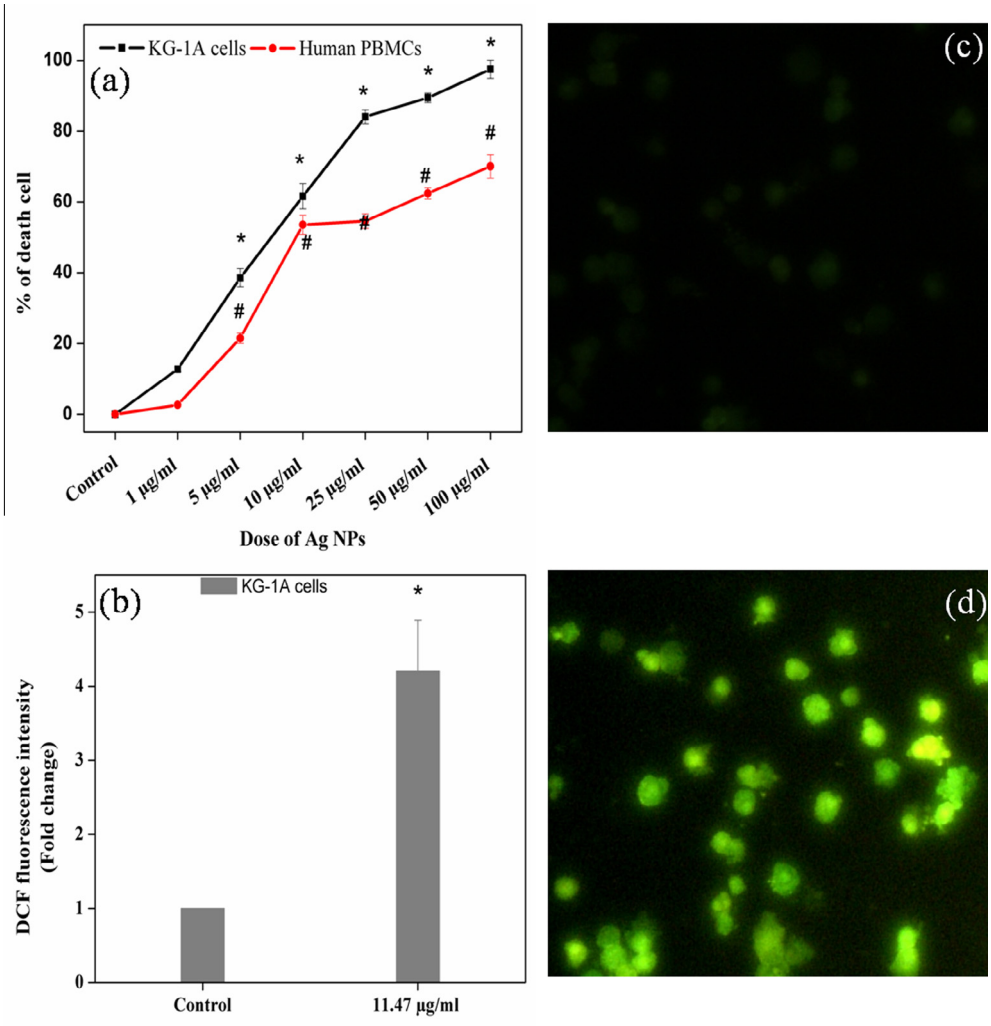

Figure 4 (a) In vitro cell proliferation assay of Ag NPs treated KG-1A cells. Values are expressed as mean ± SEM of three experiments; * indicates significant difference ($p < 0.05$) compared to the control group. (b) Measurement of ROS level in Ag NPs treated KG-1A cells. DCF fluorescence intensity was expressed in term of ROS production. Values are expressed fold change as compare with untreated cells; * indicates significant difference ($p < 0.05$) compared to the control group. Intensity of control cells were set to 1. Qualitative characterization of reactive oxygen species formation by $DCFH_2$-DA staining using fluorescence microscopy. (c) Untreated KG-1A cells. (d) KG-1A cells treated with 11.47 µg/mL Ag NPs.

study, elevated levels of ROS due to Ag NPs exposure, may lead to the failure of cellular anti oxidant defence system in KG-1A cells and thereby severe oxidative attack. Not only that, involvement of ROS can be considered as effective contribution of apoptosis underlying the etiology of cell death [20].

3.10. Role of NAC in Ag NPs mediated cytotoxicity

This experiment was performed to determine the potential role of ROS in cancer cell death induced by Ag NPs. Fig. S7 shows that pre treatment with 10 mM NAC significantly prevented the NP induced cytotoxicity and the cell viability was restored >90%. Studies showed that elevated levels of ROS stimulate the release of different pro-inflammatory markers, especially TNF-α [67]. This TNF-α intern activates NF-κB and c-Jun N-terminal kinase (c-Jun NH2-terminal kinase, JNK), which ultimately manifest cell death by activating apoptotic and necrotic pathways [68,33]. The result obtained from the experiment clearly suggested that ROS generation played a crucial role in Ag NP-induced cytotoxicity in KG-1A cells (Fig. 4b).

3.11. Cellular morphology analysis by Acridine orange (AO)–ethidium bromide (EtBr) double staining

Acridine orange (AO)–ethidium bromide (EtBr) double staining is one of the useful technique for measurement of the cellular morphology during cell death by apoptosis or necrosis. Fig. 5(a) and (b) show the results obtained from AO – EtBr double staining of KG-1A cells after Ag NPs treatment. This staining helps to visualize several distinct characteristics of viable, early apoptotic, late apoptotic and necrotic or dead cells. The viable cells which have intact DNA and nuclei have a round and green nucleus while early apoptotic cells have fragmented DNA, which appears as several green-colored nuclei. In late apoptotic and necrotic cell, the DNA is

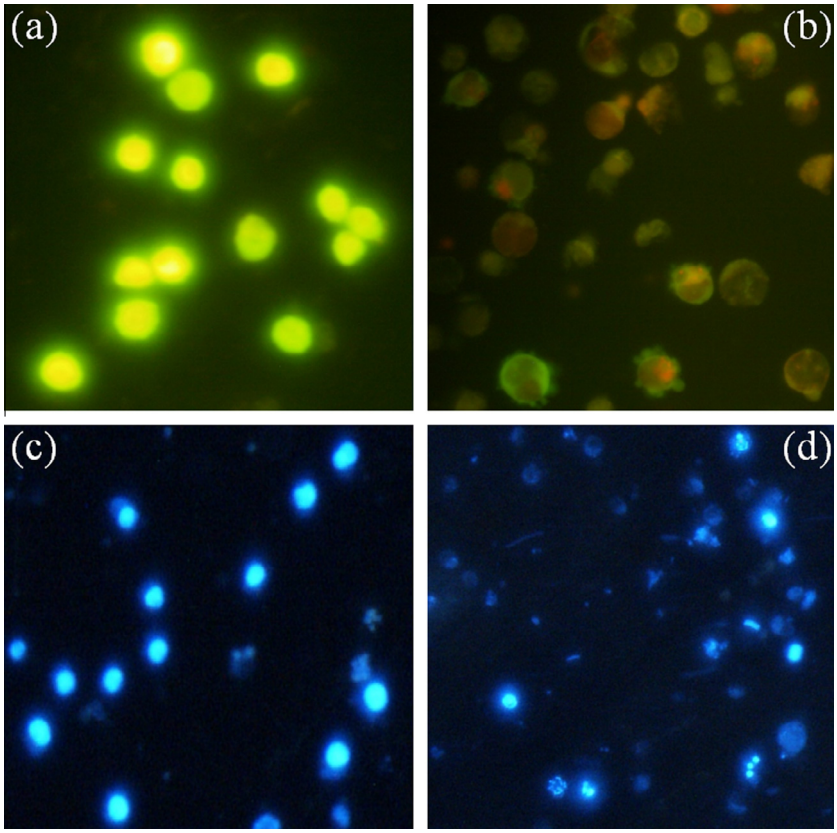

Figure 5 Morphology study of KG-1A cells treated with Ag NPs. After the treatment with nanoparticles, cells were stained with AO–EtBr and visualized under fluorescence microscope. Here, (a) untreated KG-1A cells, (b) KG-1A cells treated with Ag NPs. Qualitative characterization nuclear morphology by DAPI staining using fluorescence microscopy. After the treatment schedule with Ag NPs KG-1A cells were incubated with DAPI. At the end of DAPI exposure, cells were washed with PBS and they were visualized by fluorescence microscopy at excitation 330–380 nm and emission 430–460 nm. Here, (c) KG-1A control, (d) KG-1A cells treated with AG NPs.

fragmented and stained orange and red respectively [33]. From the fluorescence images, it is clear that Ag NPs showed significant apoptotic effects against KG-1A cells. Most of the cells showed typical characteristics of apoptosis, like plasma membrane blebbing and formation of apoptotic bodies. Maximum population of KG-1A cells were in late apoptotic phase after Ag NPs exposure. A minimum number of cells are stained red. These results indicate that most of the cells are not undergoing necrosis and cell death occurs primarily through apoptosis [35].

3.12. Detection of chromosome condensation by DAPI staining

Typical characteristics of chromatin condensation as benchmark event of apoptosis were also examined by DAPI staining (Fig. 5c and d). When KG-1A cells were treated with selected dose of Ag NPs for 24 h, chromatin condensation and fragmentation was observed in the treated group. Chromatin condensation/fragmentation in KG-1A cells suggest that Ag NPs causes cell death by induction of apoptotic process and the particles deserved potential genotoxic effects.

4. Conclusions

The present study established the bio-reductive synthesis of nano-sized Ag particles using simple water extract of *B. monosperma* bark. This easily available natural ingredient formed spherical Ag nanoparticles. Water-soluble organics present in the plant material were primarily liable for the reduction as well as stabilization of Ag ions to nano-sized metallic Ag particles, as confirmed by FTIR spectroscopic study. Size and shape of nano-level particles was studied using HRTEM and DLS measurements. XRD pattern confirmed the face-centred cubic lattice structure of the silver nanocrystals. The synthesized nanoparticles showed very efficient bactericidal effect against both type of Gram-stained bacteria. The silver nanoparticles prepared in this way also showed reasonable anticancerous activity. All these results demonstrate that the bio-ingredients present in the plant extract was effective for the synthesis of Ag nanoparticles with antibacterial and anticancerous activity. The results revealed the potent anticancer activity of Ag NPs against the KG-1A cell line. Elevation of ROS in Ag NP-exposed KG-1A cells suggests the possible contribution of apoptosis in the etiology of cell death. The AO – EtBr double staining also confirms the involvement of apoptosis rather than necrosis. These Ag NPs have great promise as anticancer agents. However, in vivo study is necessary to enlighten the effect of Ag NPs in system level. The application of Ag NPs based on these findings may lead to valuable discoveries in anticancer drug. Thus, these extract stabilized nanoparticles can be a potential candidate having various biomedical applications.

Please cite this article in press as: S. Pattanayak et al. *Butea monosperma* bark extract mediated green synthesis of silver nanoparticles: Characterization and biomedical applications, Journal of Saudi Chemical Society (2015), http://dx.doi.org/10.1016/j.jscs.2015.11.004

Acknowledgements

Authors S. Pattanayak and M.M.R. Mollick would like to express their gratitude to DST, Government of India for continuous support through INSPIRE fellowship and CRNN, Kolkata and DST-FIST for instrumental facilities. The author is also grateful to CSIR for funding support.

Appendix A. Supplementary data

Supplementary data associated with this article can be found, in the online version, at http://dx.doi.org/10.1016/j.jscs.2015.11.004.

References

[1] S.P. Dubey, M. Lahtinen, H. Särkkä, M. Sillanpää, Bioprospective of *Sorbus aucuparia* leaf extract in development of silver and gold nanocolloids, Colloids Surf. B Biointerfaces 80 (2010) 26–33.
[2] D. Mubarak Ali, N. Thajuddin, K. Jeganathan, M. Gunasekaran, Plant extract mediated synthesis of silver and gold nanoparticles and its antibacterial activity against clinically isolated pathogens, Colloids Surf. B Biointerfaces 85 (2011) 360–365.
[3] A. Ishijima, T. Yanagida, Single molecule nanobioscience, Trends Biochem. Sci. 26 (2001) 438–444.
[4] N. Ahmad, S. Sharma, Md.K. Alam, V.N. Singh, S.F. Shamsi, B.R. Mehta, A. Fatma, Rapid synthesis of silver nanoparticles using dried medicinal plant of basil, Colloids Surf. B Biointerfaces 81 (2010) 81–86.
[5] Md.M.R. Mollick, B. Bhowmick, D. Maity, D. Mondal, I. Roy, J. Sarkar, D. Rana, K. Acharya, S. Chattopadhyay, D. Chattopadhyay, Green synthesis of silver nanoparticles-based nanofluids and investigation of their antimicrobial activities, Microfluid. Nanofluid. 16 (2014) 541–551.
[6] A. Singh, D. Jain, M.K. Upadhyay, N. Khandelwal, H.N. Verma, Green synthesis of silver nanoparticles using *Argemone mexicana* leaf extract and evaluation of their antimicrobial activities, Dig. J. Nanomater. Biostruct. 5 (2010) 483–489.
[7] A. Rai, A. Singh, A. Ahmad, M. Sastry, Role of halide ions and temperature on the morphology of biologically synthesized gold nanotriangles, Langmuir 22 (2006) 736–741.
[8] P.S. Retchkiman-Schabes, G. Canizal, R. Becerra-Herrera, C. Zorril-la, H.B. Liu, J.A. Ascencio, Biosynthesis and characterization of Ti/Ni bimetallic nanoparticles, Opt. Mater. 29 (2006) 95–99.
[9] H. Gu, P.L. Ho, E. Tong, L. Wang, B. Xu, Presenting vancomycin on nanoparticles to enhance antimicrobial activities, Nano Lett. 3 (2003) 1261–1263.
[10] Z. Ahmad, R. Pandey, S. Sharma, G.K. Khuller, Alginate nanoparticles as antituberculosis drug carriers: formulation development, pharmacokinetics and therapeutic potential, Indian J. Chest Dis. Allied Sci. 48 (2005) 171–176.
[11] D. Maity, M.M.R. Mollick, D. Mondal, B. Bhowmick, M.K. Bain, K.P. Bankura, J. Sarkar, K. Acharya, D. Chattopadhyay, Synthesis of methylcellulose–silver nanocomposite and investigation of mechanical and antimicrobial properties, Carbohydr. Polym. 90 (2012) 1818–1825.
[12] K.P. Bankura, D. Maity, M.M.R. Mollick, D. Mondal, B. Bhowmick, M.K. Bain, A. Chakraborty, J. Sarkar, K. Acharya, D. Chattopadhyay, Synthesis, characterization and antimicrobial activity of dextran stabilized silver nanoparticles in aqueous medium, Carbohydr. Polym. 89 (2012) 1159–1165.
[13] M.A. Farooqui, P.S. Chauhan, P. Krishnamoorthy, J. Shaik, Extraction of silver nano-particles from the leaf extracts of Clerodendrum inearme, Dig. J. Nanomater. Biostruct. 5 (2010) 43–49.
[14] K.P. Upendra, S.S. Preeti, S. Anchal, Bioinspired synthesis of silver nanoparticles, Dig. J. Nanomater. Biostruct. 4 (2009) 159–166.
[15] K. Cho, J. Park, T. Osaka, S. Park, The study of antimicrobial activity and preservative effects of nanosilver ingredient, Electrochim. Acta 51 (2005) 956–960.
[16] H. Palza, Antimicrobial polymers with metal nanoparticles, Int. J. Mol. Sci. 16 (2015) 2099–2116.
[17] A. Šileikaitè, I. Prosyčevas, J. Puišo, A. Juraitis, A. Guobiené, Analysis of silver nanoparticles produced by chemical reduction of silver salt solution, Mater. Sci. 12 (2006) 287–291.
[18] E.K. Elumalai, T.N.V.K.V. Prasad, J. Hemachandran, S.V. Therasa, T. Thirumalai, E. David, Extracellular synthesis of silver nanoparticles using leaves of *Euphorbia hirta* and their antibacterial activities, J. Pharm. Sci. Res. 2 (2010) 549–554.
[19] M. Safaepour, A.R. Shahverdi, H.R. Shahverdi, M.R. Khorramizadeh, A.R. Gohari, Green synthesis of small silver nanoparticles using geraniol and its cytotoxicity against Fibrosarcoma-Wehi 164, Avicenna J. Med. Biotechnol. 1 (2009) 111–115.
[20] M. Jeyaraj, G. Sathishkumar, G. Sivanandhan, D. Mubarak Ali, M. Rajesh, R. Arun, G. Kapildev, M. Manickavasagam, N. Thajuddin, K. Premkumar, A. Ganapathi, Biogenic silver nanoparticles for cancer treatment: an experimental report, Colloids Surf. B Biointerfaces 106 (2013) 86–92.
[21] M.A. Franco-Molina, E. Mendoza-Gamboa, C.A. Sierra-Rivera, R.A. Gómez-Flores, P. Zapata-Benavides, P. Castillo-Tello, J.M. Alcocer-González, D.F. Miranda-Hernández, R.S. Tamez-Guerra, C. Rodríguez-Padilla, Antitumor activity of colloidal silver on MCF-7 human breast cancer cells, J. Exp. Clin. Cancer Res. 29 (2010) 148.
[22] S. Gurunathan, J. Raman, S.N.A.B.D. Malek, P.A. John, S. Vikineswary, Green synthesis of silver nanoparticles using Ganoderma neo-japonicum Imazeki: a potential cytotoxic agent against breast cancer cells, Int. J. Nanomed. 8 (2013) 4399–4413.
[23] N. Miura, Y. Shinohara, Cytotoxic effect and apoptosis induction by silver nanoparticles in HeLa cells, Biochem. Biophys. Res. Commun. 390 (2009) 733–737.
[24] Y.H. Hsin, C.F. Chen, S. Huang, T.S. Shih, P.S. Lai, P.J. Chueh, The apoptotic effect of nanosilver is mediated by a ROS- and JNK-dependent mechanism involving the mitochondrial pathway in NIH3T3 cells, Toxicol. Lett. 179 (2008) 130–139.
[25] P.V. Asha Rani, G. Low Kah Mun, M.P. Hande, S. Valiyaveettil, Cytotoxicity and genotoxicity of silver nanoparticles in human cells, ACS Nano 3 (2009) 279–290.
[26] P. Sanpui, A. Chattopadhyay, S.S. Ghosh, Induction of apoptosis in cancer cells at low silver nanoparticle concentrations using chitosan nanocarrier, ACS Appl. Mater. Interfaces 3 (2011) 218–228.
[27] R. Sukirtha, K. Priyanka, J.J. Antony, S. Kamalakkannan, R. Thangam, P. Gunasekaran, et al, Cytotoxic effect of green synthesized silver nanoparticles using *Melia azedarach* against in vitro HeLa cell lines and lymphoma mice model, Process Biochem. 47 (2012) 273–279.
[28] R. Hu, K.T. Yong, I. Roy, H. Ding, S. He, P.N. Prasad, Metallic nanostructures as localized plasmon resonance enhanced scattering probes for multiplex dark field targeted imaging of cancer cells, J. Phys. Chem. C Nanomater. Interfaces 113 (2009) 2676–2684.
[29] N.M. Dimitrijevic, D.M. Bartels, C.D. Jonah, K. Takahashi, T. Rajh, Radiolytically induced formation and optical absorption spectra of colloidal silver nanoparticles in supercritical ethane, J. Phys. Chem. B 105 (2001) 954–959.

[30] B. Yin, H. Ma, S. Wang, S. Chen, Electrochemical synthesis of silver nanoparticles under protection of poly(N-vinylpyrrolidone), J. Phys. Chem. B. 107 (2003) 8898–8904.
[31] A. Callegari, D. Tonti, M. Chergui, Photochemically grown silver nanoparticles with wavelength-controlled size and shape, Nano Lett. 3 (2003) 1565–1568.
[32] R.R. Naik, S.J. Stringer, G. Agarwal, S.E. Jones, M.O. Stone, Biomimetic synthesis and patterning of silver nanoparticles, Nat. Mater. 1 (2002) 169–172.
[33] N.G. Ntalli, F. Cottiglia, C.A. Bueno, L.E. Alche, M. Leonti, S. Vargiu, et al, Cytotoxic tirucallane triterpenoids from Melia azedarach fruits, Molecules 15 (2010) 5866–5877.
[34] S.K. Dash, S. Chattopadhyay, S. Tripathy, S.S. Dash, B. Das, D. Mandal, B.G. Bag, S. Roy, Betulinic acid, a natural bio-active compound: proficient to induce programmed cell death in human myeloid leukemia, World J. Pharm. Pharm. Sci. 3 (2014) 1348–1374.
[35] D. Guo, L. Zhu, Z. Huang, H. Zhou, Y. Ge, W. Ma, J. Wu, X. Zhang, X. Zhou, Y. Zhang, Y. Zhao, N. Gu, Anti-leukemia activity of PVP-coated silver nanoparticles via generation of reactive oxygen species and release of silver ions, Biomaterials 34 (2013) 7884–7894.
[36] A.M. Awwad, N.M. Salem, Green synthesis of silver nanoparticles by mulberry leaves extract, Nanosci. Nanotechnol. 2 (2012) 125–128.
[37] N. Samadi, D. Golkaran, A. Eslamifar, H. Jamalifar, M.R. Fazeli, F.A. Moshseni, Intra/extracellular biosynthesis of silver nanoparticles by an autochthonous strain of *Proteus mirabilis* isolated from photographic waste, J. Biomed. Nanotechnol. 5 (2009) 247–253.
[38] R. Varshney, A.N. Mishra, S. Bhadauria, M.S. Gaur, A novel microbial route to synthesize silver nanoparticles using fungus *Hormoconis resinae*, Dig. J. Nanomater. Biostruct. 4 (2009) 349–355.
[39] M. Kowshik, S. Ashtaputre, S. Kharraz, W. Vogel, J. Urban, S. K. Kulkarni, K.M. Paknikar, Extracellular synthesis of silver nanoparticles by a silver-tolerant yeast strain MKY3, Nanotechnology 14 (2003) 95.
[40] J.L. Gardea-Torresdey, J.G. Parsons, K. Dokken, J.R. Peralta-Videa, H. Troiani, P. Santiago, M. Jose-Yacaman, Formation and growth of Au nanoparticles inside live alfalfa plants, Nano Lett. 2 (2002) 397–401.
[41] J.L. Gardea-Torresdey, E. Gomez, J.R. Peralta-Videa, J.G. Parsons, H. Troiani, M. Jose-Yacaman, Alfalfa sprouts: a natural source for the synthesis of silver nanoparticles, Langmuir 19 (2003) 1357–1361.
[42] S.P. Chandran, M. Chaudhary, R. Pasricha, et al, Synthesis of gold nanotriangles and silver nanoparticles using Aloe vera plant extract, Biotechnol. Progr. 22 (2006) 577–583.
[43] M. Sathishkumar, K. Sneha, S.W. Won, et al, *Cinnamon zeylanicum* bark extract and powder mediated green synthesis of nano-crystalline silver particles and its bactericidal activity, Colloids Surf. B Biointerfaces 73 (2009) 332–338.
[44] D. Jain, H. Kumar daima, S. Kachhwaha, S.L. Kothari, Synthesis of plant-mediated silver nanoparticles using papaya fruit extract and evaluation of their anti microbial activities, Dig. J. Nanomater. Biostruct. 4 (2009) 557–563.
[45] N. Ahmad, S. Sharma, V.N. Singh, S.F. Shamsi, A. Fatma, B.R. Mehta, Biosynthesis of silver nanoparticles from *Desmodium triflorum*: a novel approach towards weed utilization, Biotechnol. Res. Int. 1 (2011) 454090.
[46] Z. Zaheer, Rafiuddin, Bio-conjugated silver nanoparticles: From *Ocimum sanctum* and role of cetyltrimethyl ammonium bromide, Colloids Surf. B Biointerfaces 108 (2013) 90–94.
[47] J. Huang, Q. Li, D. Sun, Y. Lu, Y. Su, X. Yang, H. Wang, Y. Wang, W. Shao, N. He, J. Hong, C. Chen, Biosynthesis of silver and gold nanoparticles by novel sundried *Cinnamomum camphora* leaf, Nanotechnology 18 (2007) 105104.
[48] M.F. Zayed, W.H. Eisa, A.A. Shabaka, *Malva parviflora* extract assisted green synthesis of silver nanoparticles, Spectrochim. Acta Part A Mol. Biomol. Spectrosc. 98 (2012) 423–428.
[49] P.K. Stoimenov, R.L. Klinger, G.L. Marchin, K.J. Klabunde, Metal oxide nanoparticles as bactericidal agents, Langmuir 18 (2002) 6679–6686.
[50] P. Cos, A.J. Vlietinck, D.V. Berghe, L. Maes, Anti-infective potential of natural products: how to develop a stronger in vitro 'proof-of-concept', J. Ethnopharmacol. 106 (2006) 290–302.
[51] S.K. Dash, S. Chattopadhyay, T. Ghosh, S. Tripathy, S. Das, D. Das, S. Roy, Antileukemic efficacy of monomeric manganese-based metal complex on KG-1A and K562 cell lines, ISRN Oncol. (2013), http://dx.doi.org/10.1155/2013/709269. Article ID 709269.
[52] S.K. Dash, T. Ghosh, S. Roy, S. Chattopadhyay, D. Das, Zinc sulfide nanoparticles selectively induce cytotoxic and genotoxic effects on leukemic cells: involvement of reactive oxygen species and tumor necrosis factor alpha, J. Appl. Toxicol. 34 (2014) 1130–1144.
[53] K. Ho, L.S. Yazan, N. Ismail, M. Ismail, Apoptosis and cell cycle arrest of human colorectal cancer cell line HT-29 induced by vanillin, Cancer Epidemiol. 33 (2009) 155–160.
[54] M.M.R. Mollick, B. Bhowmick, D. Mondal, D. Maity, D. Rana, S.K. Dash, S. Chattopadhyay, S. Roy, J. Sarkar, K. Acharya, M. Chakraborty, D. Chattopadhyay, Anticancer (in vitro) and antimicrobial effect of gold nanoparticles synthesized using *Abelmoschus esculentus* (L.) pulp extract via a green route, RSC Adv. 4 (2014) 37838–37848.
[55] M. Sastry, K.S. Mayyaa, K. Bandyopadhyay, pH dependent changes in the optical properties of carboxylic acid derivatized silver colloidal particles, Colloids Surf. A 127 (1997) 221–228.
[56] J. Xie, J.Y. Lee, D.I.C. Wang, Y.P. Ting, Silver nanoplates: from biological to biomimetic synthesis, ACS Nano 1 (2007) 429–439.
[57] N. Saifuddin, C.W. Wong, A.A. Nur Yasumira, Rapid biosynthesis of silver nanoparticles using culture supernatant of bacteria with microwave irradiation, E-J. Chem. 6 (2009) 61–70.
[58] N. Jain, A. Bhargava, S. Majumdar, J.C. Tarafdar, J. Panwar, Extracellular biosynthesis and characterization of silver nanoparticles using *Aspergillus flavus* NJP08: a mechanism perspective, Nanoscale 3 (2011) 635–641.
[59] M.B. Ahmad, J.J. Lim, K. Shameli, N.A. Ibrahim, M.Y. Tay, Synthesis of silver nanoparticles in chitosan gelatin and chitosan/gelatin bionanocomposites by a chemical reducing agent and their characterization, Molecules 16 (2011) 7237–7248.
[60] T.P. Amaladhas, S. Sivagami, T.A. Devi, N. Ananthi, S.P. Velammal, Biogenic synthesis of silver nanoparticles by leaf extract of *Cassia angustifolia*, Adv. Nat. Sci. Nanosci. Nanotechnol. 3 (2012) 045006, 7pp.
[61] K. Kalimuthu, R.S. Babu, D. Venkataraman, M. Bilal, S. Gurunathan, Biosynthesis of silver nanocrystals by *Bacillus licheniformis*, Colloids Surf. B Biointerfaces 65 (2008) 150–153.
[62] F.-P. Gao, H.-Z. Zhang, L.-R. Liu, Y.-S. Wang, Q. Jiang, X.-D. Yang, Q.-Q. Zhang, Preparation and physicochemical characteristics of self-assembled nanoparticles of deoxycholic acid modified-carboxymethyl curdlan conjugates, Carbohydr. Polym. 71 (2008) 606–613.
[63] Y.M. Mohan, K.M. Raju, K. Sambasivudu, S. Singh, B. Sreedhar, Preparation of acacia-stabilized silver nanoparticles: a green approach, J. Appl. Polym. Sci. 106 (2007) 3375–3381.
[64] V.T.P. Vinod, P. Saravanan, B. Sreedhar, D.K. Devi, R.B. Sashidhar, A facile synthesis and characterization of Ag, Au and Pt nanoparticles using a natural hydrocolloid gum kondagogu (Cochlospermum gossypium), Colloids Surf. B 83 (2011) 291–298.

[65] A. Barth, The infrared absorption of amino acid side chains, Prog. Biophys. Mol. Biol. 74 (2000) 141–173.
[66] P. Dibrov, J. Dzioba, K.K. Gosink, C.C. Hase, Chemiosmotic mechanism of antimicrobial activity of Ag(+) in Vibrio cholerae, Antimicrob. Agents Chemother. 46 (2002) 2668–2670.
[67] K. Peters, R.E. Unger, A.M. Gatti, E. Sabbioni, R. Tsaryk, C. Kirkpatrick, Metallic nanoparticles exhibit paradoxical effects on oxidative stress and pro-inflammatory response in endothelial cells in vitro, Int. J. Immunopathol. Pharmacol. 20 (2007) 685–695.
[68] H.M. Shen, S. Pervaiz, TNF receptor superfamily-induced cell death: redoxdependent execution, FASEB J. 20 (2006) 1589–1598.